

### 33. CHROMIUM-BEARING SPINELS IN SOME ROCKS OF LEG 45: PHASE CHEMISTRY, ZONING AND RELATION TO HOST BASALT CHEMISTRY

A. L. Graham, R. F. Symes, J. C. Bevan, and V. K. Din, Department of Mineralogy, British Museum (Natural History), London, United Kingdom

#### INTRODUCTION

The basalts obtained during Leg 45, the inaugural cruise of the International Phase of Ocean Drilling (IPOD), may be divided most simply into phyric and aphyric types. The lavas obtained from Holes 395 and 395A (which penetrated 576 m sub-basement) have been further subdivided, on chemical grounds, into a total of 10 principal units. The phyric units are designated P<sub>1</sub>-P<sub>5</sub>, the aphyric units A<sub>1</sub>-A<sub>5</sub>. This aspect of the basalts is discussed elsewhere in this volume and will be mentioned here only briefly.

This paper is concerned with the Cr-bearing spinels that constitute a rare phenocryst phase in many ocean floor basalts. In Hole 395A, they are more common in the phyric units than in the aphyric basalts. Chromium-rich spinel occurs (about one grain per thin section) in only a small portion of the 207 meters of the major aphyric unit (A<sub>3</sub>); generally the aphyric basalts do not contain Cr-rich spinels. Only 34 of the 174 thin sections of Hole 395A basalts contain Cr-bearing spinel phenocrysts, and only 4 of these are from an aphyric unit (A<sub>3</sub>, Cores 43 and 46). This discussion is restricted to Hole 395A, since Cr-rich spinels have not so far been found in the 20 thin sections of basalts from Hole 395. In Hole 396, Cr-rich spinels are much more common, so much so that nearly all the thin sections examined contain at least two or three crystals. These spinels are often associated with the phenocryst phases, olivine and plagioclase, either included within them or attached to their rims. Free Cr-rich spinels as phenocrysts are less common than in Hole 395A. Data in this paper are restricted to those obtained from samples from Holes 395 and 395A.

Cr-rich spinel is an early-crystallizing phase from a basaltic fluid containing around 300 ppm Cr; ocean-floor basalts generally have between 200 and 400 ppm Cr, and might be expected to contain this phase. In the basalts of Hole 395A, Cr-bearing spinels occur included within magnesian olivine (~Fo<sub>88</sub>), calcic plagioclase (~An<sub>60-88</sub>), or as a free, often subhedral, phenocryst. They range in size from 0.02 mm to 0.4 mm across; the free phenocrysts are generally at the larger end of the range. Compositional zoning is common, and this is observed whether or not the spinel is apparently within a phenocryst.

#### RESULTS

Table 1 gives representative analyses of Cr-bearing spinels from Holes 395 and 395A, and each analysis is

related to the magma type of its host rock (P<sub>2</sub>-P<sub>5</sub>, A<sub>3</sub>; see elsewhere in this volume for magma chemistry groups and their characterization). Generally, core and rim data quoted were obtained from single spinel grains, but in two cases (columns 6a, 6b and 11a, 11b), the composition range is not adequately represented by analyses from a single grain, and the maximum rim-to-core variation in a particular lava type is indicated by analyses from different grains. The cations have been calculated to 32 oxygens, with Fe<sup>3+</sup>:Fe<sup>2+</sup> proportioned so that Y = 16 (where the ideal spinel is XY<sub>2</sub>O<sub>4</sub>). Caution is needed in interpreting the Mn data: the electron microprobe used was not able to resolve the MnK $\alpha$  peak from the large CrK $\beta$  peak, and a portion of the Mn signal from the spinels was due to Cr. Thus a portion of the MnO reported in Table 1 is due to Cr interference on the Mn peak. One estimate of addition to the Mn signal suggests that it is about 2 per cent of the Cr present in the spinel.

#### DISCUSSION

The concentration of Cr in the lavas of Hole 395A varies with lava type: between 200 ppm (P<sub>2</sub>) and 370 ppm (P<sub>3</sub>, A<sub>3</sub>). In the P<sub>3</sub> and P<sub>4</sub> lavas, the Cr-rich spinel often is accompanied by Cr-rich diopside (~1.9% Cr<sub>2</sub>O<sub>3</sub>), so in this part of the drilled core a proportion of the bulk Cr is in the pyroxenes. Indeed, the Cr-rich spinels occasionally contain siliceous vermicular "inclusions" in their outer parts, which suggest that the spinel is actively reacting with the liquid. This seems to occur only where a Cr-rich diopside is also present, though all the phenocryst Cr-rich spinels are rounded to some extent.

The partition coefficient for Cr between spinel and basaltic liquid so favors spinel that under experimental conditions (Hill and Roeder, 1974) Cr-rich spinel crystallized from melts containing only 80 ppm Cr. It is odd therefore that mid-ocean ridge basalts, with characteristically between 200 ppm and 400 ppm Cr, should not contain greater modal proportions of spinel. In the Leg 34 (Nazca plate) basalts, Cr-rich spinel is apparently very rare, even though the basalts contain ~300 ppm Cr, whereas in Leg 37 basalts from the Mid-Atlantic Ridge they are much more common (Sigurdsson, 1977). Sigurdsson and Schilling (1976) suggest that lavas containing less than 400 ppm Cr do not in general contain Cr-rich spinel: this does not seem to be the case in this work, nor does there seem to be any chemical reason why it should be so. The data of Hill and Roeder (1974) suggest a maximum

TABLE 1  
Electron Microprobe Analyses of Cr-Bearing Spinels in Rocks From Holes 395 and 395A (compositions in wt %)

Magma Type Hole 395 Specimen 1	P2 395A		P3		P3		P3		P4	P4	P4	P5		P5		P5		A3		
	Core	Rim	Core	Rim	Core	Rim	Core	Rim	6a Core	6b Rim	7	Core	Rim	Core	Rim	Core	Rim	11a Core	11b Rim	
TiO <sub>2</sub>	0.11	0.37	0.37	0.63	0.96	0.72	0.35	0.66	0.83	0.62	1.45	0.72	0.56	0.63	0.59	0.79	0.58	4.73	0.61	0.75
Al <sub>2</sub> O <sub>3</sub>	33.53	40.63	40.09	24.54	22.61	28.74	25.95	27.38	26.14	26.49	23.35	31.00	38.88	36.07	27.48	25.64	31.94	21.02	28.71	28.41
Cr <sub>2</sub> O <sub>3</sub>	34.00	23.98	24.25	40.17	38.14	35.23	37.31	37.48	36.16	39.14	36.30	34.45	26.39	28.41	37.88	37.41	32.15	31.69	39.46	39.22
FeO	15.57	14.29	17.08	19.55	24.11	20.18	20.73	18.55	21.41	18.18	31.16	18.04	16.63	16.98	16.92	23.54	19.00	33.55	14.10	18.68
MnO	0.68	0.37	0.46	0.73	0.81	0.58	0.67	0.66	0.68	0.60	0.76	0.51	0.21	0.23	0.61	0.64	0.66	0.81	0.67	0.72
MgO	15.43	19.27	17.09	14.35	11.54	14.62	14.16	15.25	13.32	14.98	6.79	15.06	16.25	15.97	16.43	12.53	14.67	8.39	16.93	13.55
Total	99.32	98.91	99.34	99.97	98.17	100.07	99.17	99.98	98.54	100.01	99.81	99.78	98.92	98.29	99.91	100.55	99.00	100.19	100.48	101.33
Ti	0.020	0.063	0.063	0.116	0.185	0.130	0.065	0.120	0.168	0.111	0.283	0.128	0.097	0.111	0.105	0.144	0.104	0.925	0.108	0.134
Al	9.273	10.807	10.775	7.102	6.839	8.158	7.546	7.786	7.656	7.472	7.141	8.677	10.536	9.959	7.648	7.328	9.002	6.440	7.959	7.979
Cr	6.308	4.278	4.371	7.797	7.738	6.711	7.281	7.148	7.103	7.406	7.446	6.471	4.797	5.261	7.072	7.173	6.081	6.512	7.337	7.388
Fe <sup>3+</sup>	0.399	0.852	0.791	0.985	1.238	1.001	1.108	0.946	1.073	1.011	1.130	0.724	0.570	0.669	1.175	1.355	0.813	2.123	0.596	0.499
Fe <sup>2+</sup>	2.656	1.845	2.466	3.030	3.937	3.065	3.171	2.797	3.376	2.627	5.631	2.860	2.628	2.658	2.167	3.418	2.988	5.171	2.175	3.224
Mg	5.396	6.480	5.808	5.251	4.414	5.252	5.211	5.483	4.933	5.342	2.626	5.335	5.568	5.575	5.780	4.529	5.232	3.250	5.934	4.812
Mn	0.135	0.071	0.089	0.152	0.176	0.118	0.140	0.135	0.143	0.030	0.167	0.103	0.041	0.046	0.047	0.052	0.134	0.178	0.133	0.145
Mg/ Mg+Fe <sup>2+</sup>	0.67	0.78	0.70	0.63	0.53	0.63	0.62	0.66	0.59	0.67	0.32	0.65	0.68	0.68	0.72	0.57	0.64	0.39	0.73	0.60

Note: 1 = 18-1, 74-75 cm (#2D); 2 = 14-1, 90-100 cm (#12); 3 = 20-1, 142-144 cm (#11); 4 = 22-1, 92-94 cm (#13B); 5 = 22-1, 87-92 cm (#13A); 6a = 26-2, 25-33 cm (#1C); 6b = 22-2, 72-76 cm (#4D); 7 = 61-1, 120-122 cm (#2A); 8 = 31-1, 83-87 cm (#6); 9 = 29-1, 143-148 cm (#5); 10 = 31-1, 70-70 cm (#4); 31-1, 70-76 cm (#4); 11a = 43-1, 132-134 cm (#3); 11b = 46-1, 41-43 cm (#1).

solubility of Cr in the liquid of between 200 and 300 ppm, and also that the lower the Cr content of the liquid the lower the liquidus temperature of the Cr-rich spinel (at a fixed  $P_{O_2}$ ). A possible result of the latter finding is that the clinopyroxene liquidus may be intersected before that of the Cr-rich spinel. Once this has happened, it is less likely that the spinel will be precipitated, since the clinopyroxene contains more Cr than the liquid, and the nucleation of Cr-rich spinel is inhibited.

Petrographic observations indicate that the Cr-rich spinels are not inert, and that once formed they react with the residual liquid. This is suggested by the subhedral outline of the crystals, whether or not they are within other phenocryst phases, either olivine or plagioclase. Analyses (Table 1) show that the early-formed spinels have reacted and exchanged divalent and trivalent cations with the liquid. The amount of trivalent ion exchange is more limited than that of the divalent ions; indeed, the range in  $Y_{Sp}^{Cr}$  ( $\equiv$  mol Cr: (Cr + Al + Fe<sup>3+</sup>) in the spinel) is restricted (0.51 to 0.27; see Figure 2), despite large changes in the  $X_{Sp}^{Mg}$  (mol Mg: (Mg + Fe<sup>2+</sup>) in the spinel, (0.78 to 0.23; see Figure 2 and 3[b]). There seems to be no trend in  $Y_{Sp}^{Fe^{3+}}$  of the spinel cores which suggests for them a primitive character. The  $Y_{Sp}^{Cr}$  variation is, in general, less than 2 per cent, with only rare excursions beyond this; see Figure 4. The variation in Ti, however, is often a sensitive indicator of Mg/Fe zoning, so that a fraction of the Y cations must be exchanging with the liquid to relatively low temperatures. It appears that the two exchange reactions, one involving divalent ions, Mg and Fe<sup>2+</sup>, and the other involving trivalent ions, Fe<sup>3+</sup>, Al, Cr, can occur independently of one another. The trend of the zoning in Y<sup>3+</sup> is to higher Cr contents with decreasing  $X_{Sp}^{Mg}$ , though this is not invariably so. Rarely this covariation is reversed, particularly in the "cores" of the spinels. Here the Al content rises slightly before the dominant trend of Cr increase asserts itself. Generally the major zonation is in Mg:Fe.

Despite the similarity in the major element chemistry of the phryic lavas of Hole 395A (Table 2 and

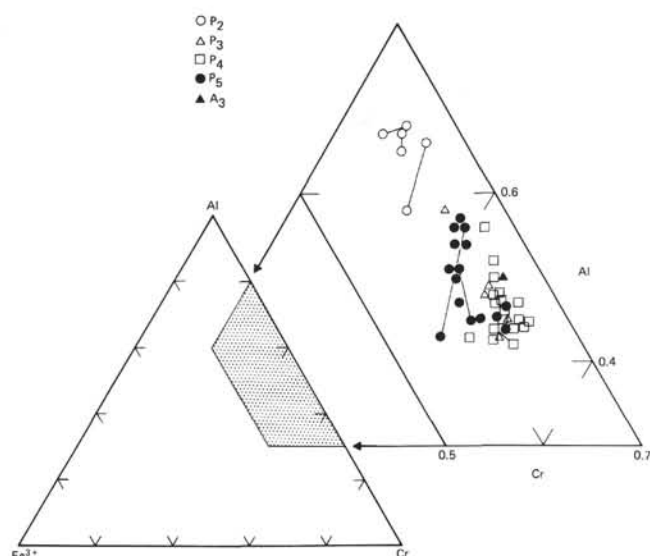


Figure 1. Ternary plot of the molecular proportions of  $Y^{3+}$  (Al, Cr, Fe<sup>3+</sup>) in the analyzed spinels. The lines join core and rim compositions; the more aluminous of the two is that of the core. The symbols designate the magma type.

elsewhere in this volume), the spinel composition can be related to that of the host lava in terms of the proportions of the trivalent ions (e.g.,  $Y_{Sp}^{Cr}$ ), in the following order:

$$\frac{P_2 - P_5 - P_3, P_4}{\text{increasing } Y_{Sp}^{Cr}}$$

However, since the bulk alumina contents of these lavas are very similar [ $P_2 \sim 18.0\%$  Al<sub>2</sub>O<sub>3</sub> (wt),  $P_5 \sim 18.3\%$ ,  $P_3 \sim 17.7\%$ ,  $P_4 \sim 17.1\%$ ], the correlation between Al<sub>2</sub>O<sub>3</sub> in the spinel and Al<sub>2</sub>O<sub>3</sub> content of the host lava is weak, but the trend is for the least aluminous spinels to occur in the least aluminous lava. Since this trend,  $P_2-P_5-P_3, P_4$ , is also that of increas-

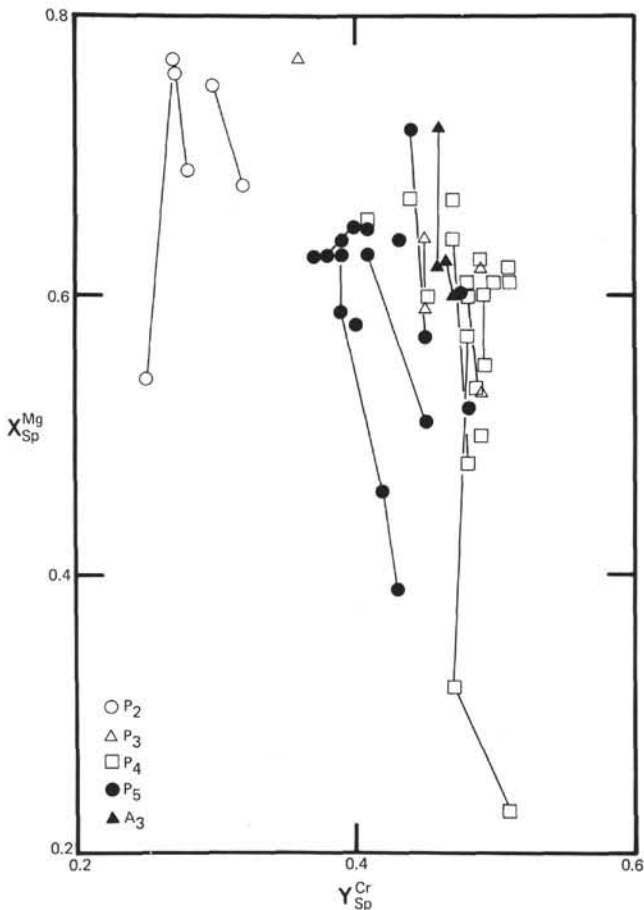


Figure 2.  $X_{Sp}^{Mg}$  [= mol Mg: (Mg+Fe<sup>2+</sup>)] plotted against  $Y_{Sp}^{Cr}$  [= mol Cr: (Cr+Al+Fe<sup>3+</sup>)] for the Cr-bearing spinels occurring as phenocrysts in basalts from Hole 395A. The lines join core and rim compositions; the more magnesian of the two is that of the core. The symbols designate the magma type, as indicated.

ing Cr concentration in the lava, it may be that the prime factor dictating the spinel  $Y^{3+}$  proportions is Cr availability, not the  $Al_2O_3$  content, which, in the lava, is much in excess of that needed for spinel formation.

Sigurdsson (1977) has shown that for Cr-rich spinels in Leg 37 rocks there is a correlation between the  $Al_2O_3$  content of the rock and that of the spinel; but it is more likely that the Cr content of the lava controls the spinel composition, and that aluminum takes a passive role. For the Hole 395A lavas, the correlation between the Cr content of the lava and  $Y_{Sp}^{Cr}$  is much better than the alumina correlation.

There is no correlation between  $X_{Sp}^{Mg}$  and Mg:(Mg + Fe<sup>2+</sup>) of the host basalt, which might suggest that the Cr-rich spinels are xenocrysts in their present host lavas. In fact this is only rarely the case. Some coexisting olivine-Cr-rich spinel pairs have been analyzed, and a plot of  $\ln K_D$  against  $Y_{Sp}^{Cr}$  (following Irvine, 1965) is given in Figure 5. In general, the majority of these pairs plot in a restricted area. The line drawn is that of maximum slope passing through the origin and the center of the field of plotted points. For equilib-

rium, the intercept on the  $\ln K_D$  axis must be greater than 0 (see Irvine, 1965), but the scatter of points and the lack of definitive lineation does not define a particular intercept on  $\ln K_D$ . Two points plot well away from the main cluster and are labeled A and B. Point A is that for the olivine-spinel pair in the tectonized harzburgite from Hole 395. Point B, from a spinel-olivine pair in a P<sub>2</sub> basalt, plots well below the line and in a position which indicates that the equilibrium conditions were very different from those of the majority of the spinel-olivine pairs. This particular spinel is included within a plagioclase phenocryst: it is zoned, and has certainly attempted to equilibrate in part with a host liquid. Although the core is too magnesian to be in equilibrium with the coexisting olivine, the rim is not. The average rim composition (triangle in Figure 5) plots close to the line drawn arbitrarily on the diagram. This may well be fortuitous since most of the rim compositions give  $\ln K_D$  values which plot well above the line and are in no linear array, as would be expected if the spinel continued to equilibrate with the liquid after olivine had ceased to crystallize. In the case of the spinel-olivine pair plotted at B in Figure 5, the spinel rim is still in equilibrium with olivine, since it is included in a plagioclase phenocryst which has prevented re-equilibration with the later stage liquids. The zoning in the olivines should also reflect this continuing equilibration with falling temperature, but so far data are not available on these samples to test this, partly because most of the olivines have altered rims.

With a few exceptions the core compositions of the spinels in the lavas of Hole 395A appear to be in equilibrium with their coexisting olivine. Unfortunately, this does not exclude a xenocryst origin for both phases, initially at equilibrium under conditions very different from those in which they were incorporated into their present host. The olivine composition varies between Fo<sub>83</sub> and Fo<sub>88</sub>, with occasional values of Fo<sub>90</sub>. All these olivines have a CaO content (~0.35% by weight) quite distinct from that of the olivine in the tectonized ultramafic of Hole 395 (0.06% CaO), although the bulk composition is very similar: Fo<sub>90</sub>. Thus, the olivines in the lavas are distinguishable from olivines of ultramafic origin, as seen in Hole 395 and in the ultramafics of Leg 37 (Symes et al., 1977), by their CaO content. No olivine in the lavas has been found to have a CaO content of less than 0.28 per cent; this implies that they all crystallized from a basaltic fluid and not from an ultramafic source. By inference, the same considerations apply to the Cr-rich spinels, which must have crystallized from their basaltic hosts and are not xenocrysts in their present environment. They have not been derived from a source of ultramafic composition.

Since the spinel core compositions appear to reflect the bulk chemistry of their host lavas, the zoning observed in these spinels does depend on the residual liquid composition at various stages of crystal fractionation. The modal abundance of Cr-rich spinel is small, so that crystallization of this phase will have little effect

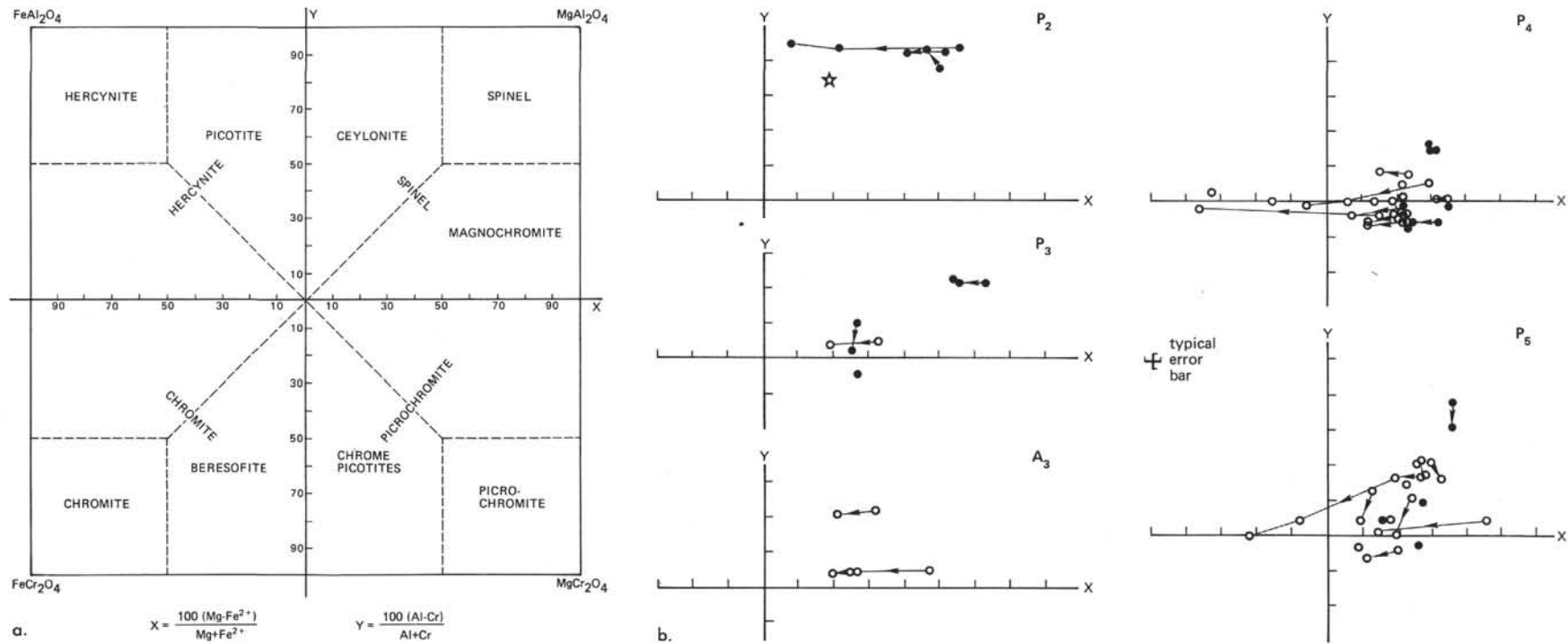


Figure 3. (a) A spinel composition plot after Simpson (1920), showing the derivation of fig. 3b. (b) Spinel plotted in the manner of Simpson (see fig. 3a and Simpson [1920]), and separated according to magma type. Filled circles = spinels within phenocrysts; open circles = spinels in groundmass; open star = spinel from tectonited harzburgite of Hole 395. Arrows indicate core-to-rim variation. Scale units on (b) same as in (a).

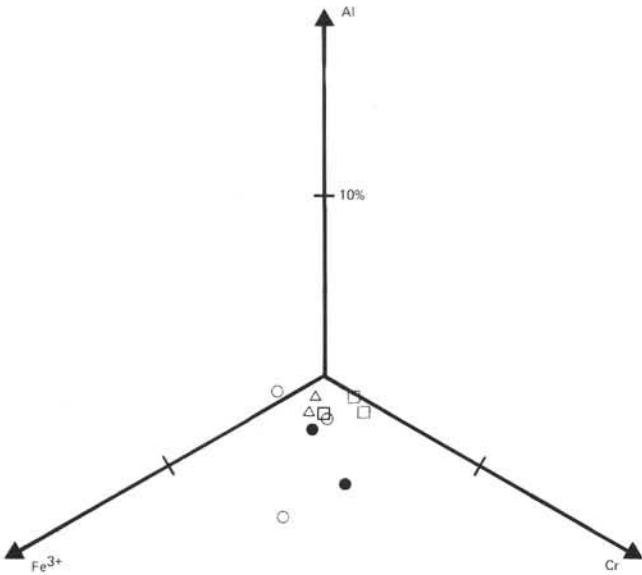


Figure 4. A three-vector plot in two dimensions of the molecular proportions of  $Y^{3+}$  in the spinels, showing the extent of core-to-rim zoning in  $Y^{3+}$ . The cores are all plotted at the intersection of the axes, and the distance of the plots from this intersection indicates the extent of zoning. Most of the spinels show a  $Y^{3+}$  variation of less than 3 per cent (molecular). Symbols same as in Figure 2.

on the liquid composition with respect to the major elements, Mg, Fe, Al, Ti, but changes in the liquid composition will be reflected in the composition of the spinel. These considerations suggest that Cr-rich spinel is a sensitive indicator of liquid compositions during the fractionation of a basaltic fluid.

REFERENCES

Hill, R. and Roeder, P., 1974. The crystallization of spinel from basaltic liquid as a function of oxygen fugacity: *J. Geol.*, v. 82, p. 709-730.  
 Irvine, T. N., 1965. Chromian spinel as a petrogenetic indicator, 1. Theory: *Canadian J. Earth Sci.*, v. 2, p. 648-672.  
 Sigurdsson, H., 1977. Spinels in Leg 37 lavas: Phase chemistry and zoning. In Aumento F., Melson, W.G., et al., *Initial Reports of the Deep Sea Drilling Project*, v. 37: Washington (U.S. Government Printing Office), p. 883-892.

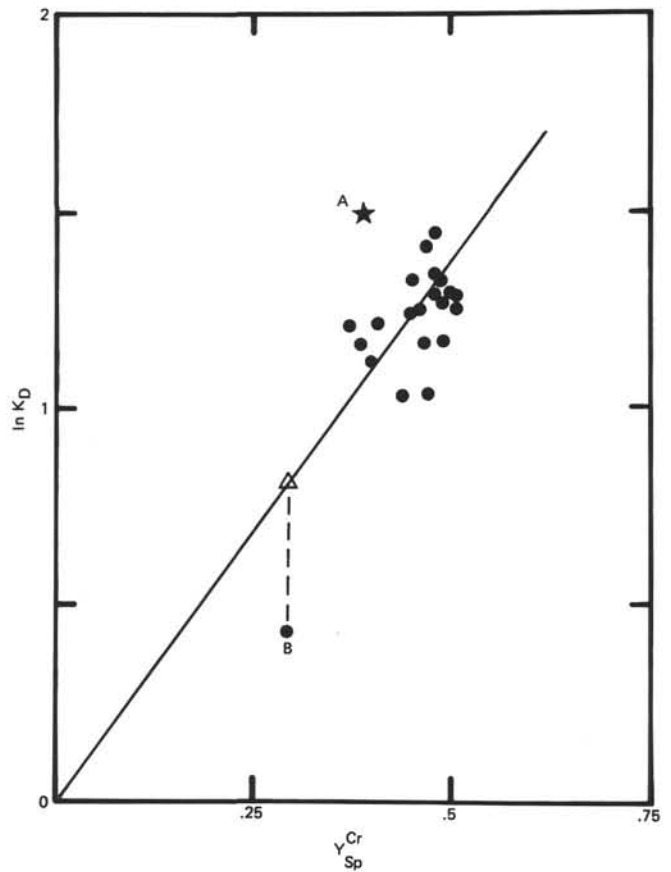


Figure 5. A plot of  $\ln K_D = \left[ \frac{X_{ol}^{Mg} X_{Sp}^{Fe}}{X_{ol}^{Fe} X_{Sp}^{Mg}} \right]$  against  $Y_{Sp}^{Cr}$ .

The line is arbitrarily drawn through  $\ln K_D = 0$ ,  $Y_{Sp}^{Cr} = 0$  and the cluster of data points. The black star A is from the tectonized harzburgite of Hole 395. For an explanation of B and the open triangle, see text.

Sigurdsson, H. and Schilling J.-G., 1976. Spinels in Mid-Atlantic Ridge basalts: Chemistry and occurrence: *Earth Planet Sci. Lett.*, v. 29, p. 7-20.  
 Simpson, E. S., 1920. A graphic method for the comparison of minerals with four variable components forming two isomorphous pairs. *Min. Mag.*, v. 19, p. 99-106.  
 Symes, R. F., Bevan, J. C., and Hutchison, R., 1977. Phase chemistry studies on gabbro and peridotite rocks from site 334, DSDP Leg 37. In Aumento, F., Melson, W. G., et al., *Initial Reports of the Deep Sea Drilling Project*, v. 37: Washington (U.S. Government Printing Office), p. 841-845.

TABLE 2  
Chemical Analysis of Samples From Sites 395 and 395A (compositions in wt %)

	Sample																			
	1	2	3	4	5 <sup>a</sup>	6 <sup>a</sup>	7	8	9 <sup>a</sup>	10 <sup>a</sup>	11	12	13	14	15	16	17	18	19	20 <sup>a</sup>
SiO <sub>2</sub>	48.8	48.9	49.0	48.8	48.0	40.8	48.8	49.2	48.8	48.7	49.1	49.3	49.6	48.7	49.6	48.5	48.6	49.3	49.7	49.4
TiO <sub>2</sub>	1.58	1.60	1.62	1.60	0.37	0.02	1.62	1.63	1.34	1.12	0.98	1.10	1.10	0.97	1.11	1.08	1.57	1.12	1.15	1.05
Al <sub>2</sub> O <sub>3</sub>	14.5	14.8	14.7	14.6	16.6	1.09	15.0	14.8	17.3	18.9	17.7	16.0	16.6	16.6	16.6	18.0	14.6	16.6	16.1	17.0
Fe <sub>2</sub> O <sub>3</sub>	3.53	2.82	3.26	2.88	1.52	4.32	3.50	2.25	2.07	1.93	3.04	2.48	3.40	2.95	2.03	3.35	4.30	1.92	3.25	1.89
FeO	7.69	8.25	7.81	8.20	4.46	4.53	7.75	9.01	6.58	5.75	4.59	5.93	4.86	4.79	6.05	4.56	5.99	6.17	5.10	5.92
MnO	0.17	0.17	0.17	0.17	0.11	0.10	0.18	0.19	0.14	0.12	0.12	0.14	0.15	0.14	0.13	0.18	0.18	0.14	0.15	0.14
MgO	8.43	8.54	8.11	8.36	11.4	40.8	8.27	8.41	7.26	7.00	7.84	8.35	7.65	8.65	8.24	7.59	8.48	8.79	8.67	8.88
CaO	10.3	10.4	10.4	10.4	8.86	0.86	10.3	10.4	11.7	11.8	12.4	12.1	12.0	12.4	11.5	12.0	10.9	11.7	11.7	11.7
Na <sub>2</sub> O	3.05	2.87	2.95	2.94	3.51	0.07	2.87	2.75	2.73	2.37	2.38	2.53	2.30	2.51	2.67	2.75	2.53	2.65	2.44	2.44
K <sub>2</sub> O	0.08	0.09	0.13	0.09	0.17	N.F.	0.16	0.15	0.11	0.07	0.09	0.11	0.15	0.10	0.06	0.16	0.23	0.08	0.11	0.07
H <sub>2</sub> O <sup>+</sup>	0.79	0.65	0.63	0.62	4.48	6.60	0.59	0.42	0.53	1.10	0.85	0.88	1.00	1.20	0.74	0.98	1.20	1.03	0.85	1.18
H <sub>2</sub> O <sup>-</sup>	0.52	0.48	0.36	0.84	0.67	0.55	0.69	0.10	0.67	0.57	0.79	0.71	0.72	0.87	0.81	1.01	1.28	0.68	0.71	0.43
P <sub>2</sub> O <sub>5</sub>	0.14	0.14	0.14	0.13	0.01	<0.01	0.14	0.14	0.13	0.11	0.09	0.12	0.09	0.07	0.11	0.10	0.14	0.10	0.10	0.09
(Total C)	0.22	0.22	0.16	0.17	0.14	0.40	0.14	0.17	0.13	0.17	0.07	0.11	0.10	0.63	0.07	0.04	0.18	0.04	0.04	0.10
"Others"	0.16	0.16	0.16	0.15	0.12	0.63	0.16	0.17	0.13	0.12	0.13	0.15	0.16	0.17	0.14	0.13	0.17	0.13	0.15	0.14
Total	99.96	100.09	99.60	99.95	100.42	100.77	100.17	99.79	99.62	100.19	100.18	99.86	100.11	100.54	100.01	100.30	100.57	100.33	100.43	100.43
Trace Elements (ppm)																				
B	5	7	2	7	7	50	3	1	3	8	9	6	N.D.	N.D.	5	8	9	4	N.F.	8
Be	<2	<2	<2	N.F.	<2	<2	<2	<2	<2	<2	<2	<2	<2	<2	<2	<2	<2	<2	<2	<2
Cr	270	270	250	270	140	2180	255	275	205	210	310	360	310	410	285	240	305	300	285	315
Li	7	7	7	7	20	<1	6	9	7	7	25	11	17	18	7	18	13	8	18	8
Nb	<5	6	7	12	<5	6	6	<5	6	N.F.	<5	N.F.	<5	<5	<5	<5	<5	<5	N.F.	6
Ni	145	140	155	125	165	2187	165	160	100	75	145	125	135	165	110	135	160	90	115	105
Co	40	45	32	35	39	70	33	55	50	41	47	44	90	95	49	44	43	40	50	55
Cu	27	17	55	13	11	28	55	75	14	10	65	48	60	65	28	60	70	6	65	14
Zn	95	105	90	95	34	60	90	95	75	65	70	70	50	45	70	70	90	70	70	60
V	300	290	280	260	190	36	270	280	230	210	200	240	270	210	200	180	270	220	230	210
Zr	105	115	115	105	<5	9	120	110	95	75	60	70	95	85	85	75	110	75	70	70
Y	39	37	38	37	11	<5	39	35	28	32	31	33	28	28	28	25	35	29	28	29
Sr	110	105	100	105	280	<5	105	115	140	140	110	95	110	120	115	140	125	115	120	120
Ba	<50	<50	<50	<50	<50	<50	<50	<50	<50	<50	<50	<50	<50	<50	<50	<50	<50	<50	<50	<50
Rb	<5	<5	<5	<5	<5	<5	<5	<5	<5	<5	<5	<5	7	<5	<5	<5	<5	<5	<5	<5
Norms																				
q	-	-	-	-	-	-	-	-	-	-	-	-	-	0.86	-	-	-	-	-	-
ne	-	-	-	-	0.48	-	-	-	-	-	-	-	-	-	-	-	-	-	-	-
or	0.47	0.53	0.77	0.53	1.00	-	0.95	0.89	0.65	0.41	0.53	0.65	0.89	0.59	0.35	0.95	1.36	0.47	0.65	0.41
ab	25.81	24.28	24.96	24.87	28.81	0.59	24.28	23.27	23.10	23.10	20.05	20.14	21.41	19.46	21.24	22.59	23.27	21.41	22.42	20.64
an	25.64	27.24	26.49	26.38	29.04	2.66	27.58	27.60	34.63	39.12	37.40	32.65	33.50	34.68	33.86	36.66	26.82	33.71	31.72	35.23
di	19.78	18.97	19.54	19.73	11.81	1.26	18.24	18.78	18.24	15.08	18.72	21.34	20.25	20.99	19.27	17.65	20.98	19.03	20.43	17.84
hy	12.28	13.59	14.11	12.62	-	24.33	14.57	15.22	10.49	9.74	15.11	15.79	14.00	13.38	15.93	9.56	14.39	12.99	14.82	14.68
ol	5.84	6.51	4.29	6.52	20.93	57.45	4.50	6.50	5.21	5.61	0.03	1.48	-	2.29	2.30	3.59	1.39	5.70	1.52	4.83
mt	5.12	4.09	4.73	4.18	2.20	6.26	5.07	3.26	3.00	2.80	4.41	3.60	4.93	4.28	2.94	4.86	6.23	2.78	4.71	2.74
il	3.00	3.04	3.08	3.04	0.70	0.04	3.08	3.10	2.54	2.13	1.86	2.09	2.09	1.84	2.11	2.05	2.98	2.13	2.18	1.99
ap	0.33	0.33	0.33	0.31	0.30	-	0.33	0.33	0.31	0.26	0.21	0.28	0.21	0.17	0.26	0.24	0.33	0.24	0.24	0.21

Note: 1 = 395-11-2, 62-64 cm; 2 = 395-12-2, 109-111 cm; 3 = 395-14-1, 131-132 cm; 4 = 395-15-1, 74-76 cm; 5 = 395-17-1, 56-59 cm; 6 = 395-18-1, 61-70 cm; 7 = 395A-7-1, 76-82 cm; 8 = 395A-8-1, 50-52 cm; 9 = 395A-15-3, 128-142 cm; 10 = 395A-15-5, 0-11 cm; 11 = 395A-22-1, 87-92 cm; 12 = 395A-22-2, 72-76 cm; 13 = 395A-25-1, 38-43 cm (#5); 14 = 395A-26-2, 24-33 cm (#1C); 15 = 395A-27-1, 127-131 cm; 16 = 395A-33-2, 9-13 cm; 17 = 395A-57-1, 125-131 cm; 18 = 395A-61-2, 37-45 cm; 19 = 395A-62-1, 80-87 cm; 20 = 395A-63-1, 108-116 cm. N.F. = Not Found. N.D. = Not Determined. "Others" includes trace elements calculated as oxides. Analytical Methods: Si, Ti, Al, Fe (Total), Mn, Mg, Ca, P, Nb, Zr, and Y: XRF analysis of fused beads prepared from 500 mg of sample + 2.000 g of lithium metaborate. FeO: Hydrofluoric/sulphuric acid dissolution followed by titration with standardized potassium permanganate [Reference: French and Adams, Analyst (London), v. 97 p. 828, 1972]. H<sub>2</sub>O<sup>-</sup>: Weight loss after 1-2 hours at 110°C. H<sub>2</sub>O<sup>+</sup> and CO<sub>2</sub> (= total carbon): using a Perkin-Elmer 240 Elemental Analyzer, samples dried at 110°C, flux added. Results corrected to "Sample as received" basis. B: Colorimetric method using curcumin (Analyst: C. J. Elliott). Remainder: Atomic absorption analysis of hydrofluoric boric acid solution of samples after Langmyhr and Paus (Reference: Anal. Chim. Acta., v. 43, p. 397, 1969).

a = Interlaboratory Standards